

# SPECTRAL PROPERTIES OF THE TWO-DIMENSIONAL MULTIWELL POTENTIAL

*N.A. Chekanov and E.V. Shevchenko*

*Belgorod State University, Belgorod, Russian Federation;  
e-mail: chekanov@bsu.edu.ru*

Two-dimensional multiwell Hamiltonian system with four local minima is considered. The motion of the system shifts from regular to chaotic through “mixed state”, i.e. the state, when regular and irregular regimes of motion coexist in different local minima. Three regimes of motion – regular ( $R$ ), mixed state ( $RC$ ), and chaotic ( $C$ ) – are considered. For each energy region the spectrum is calculated by direct diagonalization in polar coordinates, the eigenstates are classified according to the irreducible representations of the  $C_{3v}$ -point group, and the spectral statistical properties are analyzed and compared to the theoretical predictions for integrable, chaotic and generic (neither regular nor chaotic) systems.

## 1. INTRODUCTION

Searching for quantum manifestations of classical chaos has been the subject of series of investigations for the past decades [e.g. 1, 2]. The one way to do it is to analyze statistical properties of spectrum. Such investigations have been done for model systems or systems with simple topology [e.g. 3, 4]. The present research is concerned to the two-dimensional multiwell system with the Hamiltonian in the form

$$H = \frac{1}{2}(p_x^2 + p_y^2) + V(x, y), \quad (1a)$$

$$V(x, y) = \frac{1}{2}(x^2 + y^2) + b\left(x^2y - \frac{1}{3}y^3\right) + c(x^2 + y^2)^2. \quad (1b)$$

The system (1) describes surface quadrupole oscillations of a spherical drop of some matter. This system has been previously studied numerically by V. Berezovoj et al. [5]. We present here research concerning the so called “exact” eigenvalues, derived via the diagonalization procedure.

The number of critical points of the potential (1b) depends on the parameter  $W = b^2/c$ . We consider the case  $W = 18$ , so that the system (1) is multiwell with four local minima and three saddle points (cf. Fig. 1). All the minima are of the value  $V_{\min} = 0$ .

For the system (1) the transition regularity-chaos-regularity has been shown [6]. That means that the system (1) moves regularly in the region  $E < E_{cr1}$ ; invariant tori are destroyed as  $E$  approaches  $E_{cr1}$  and the motion becomes chaotic in the region  $E_{cr1} < E < E_{cr2}$ ; in the region  $E > E_{cr2}$  the regularity of the motion is recovered. In particular, for the case  $W = 18$  critical energies are found to be  $E_{cr1} \approx V_s/2$  for the central minima and  $E_{cr1} \approx V_s$  for the peripheral minima. Thus in the region  $V_s/2 < E < V_s$  regular and irregular regimes of motion coexist in different local minima. Such a phenomenon is called *mixed state*.

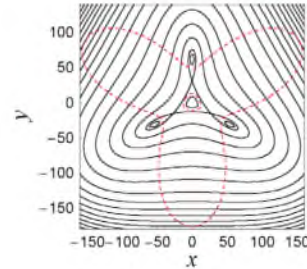


**Fig. 1.** Level lines of the potential part of the Hamiltonian (1) with  $b = 0.048$ ,  $c = 0.000128$  ( $W = b^2/c = 18$ ). Dashed lines denote the zero Gaussian curvature

We investigated the motion of the system (1) in three different regions: regular ( $R$ ) with energies  $E < V_s/2$ , mixed ( $RC$ ) with energies in the range  $V_s/2 < E < V_s$  and chaotic ( $C$ ) with  $V_s < E < E_{cr2}$ . Parameters  $b$  and  $c$  were chosen independently for each energy region in order to obtain enough energy levels for further statistical analysis (cf. Table 1).

**Table 1.** The choice of parameters  $b$  and  $c$  for investigating system (1) in energy regions  $R$ ,  $RC$ ,  $C$

Type of motion	Parameters		$E_{cr1}$	$E_s$	$E_{cr2}$
	$b$	$c$			
$R$	0.018	0.000018	385.8	868.1	1617451.8
$RC$	0.048	0.000128	54.3	122.1	227454.2
$C$	0.42	0.0098	0.7	1.5	2970.8

## 2. CLASSICAL ORBITS

The one of the commonly used ways for classifying the classical motion of the system is computation of the Poincaré surface of section pictures.

To obtain surface of section pictures shown on Fig. 2 we used the classical equations of motion for the Hamiltonian (1)

$$\ddot{x} = -x - 2bxy - 4cx(x^2 + y^2), \quad (2)$$

$$\ddot{y} = -y - b(x^2 - y^2) - 4cy(x^2 + y^2) \quad (3)$$

and the fourth-order Runge-Kutta step method for computing the classical trajectories.

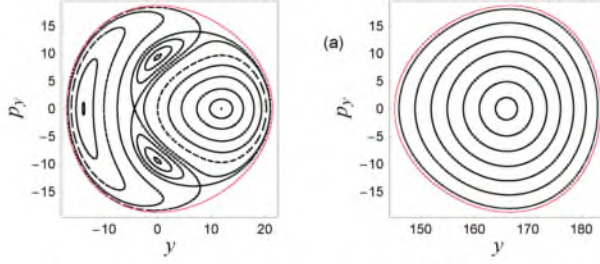


**Fig. 2,a.** Type of motion  $R$ .  $E = 175.0$ . Shown is the surface of section for central (left) and peripheral (right) local minima

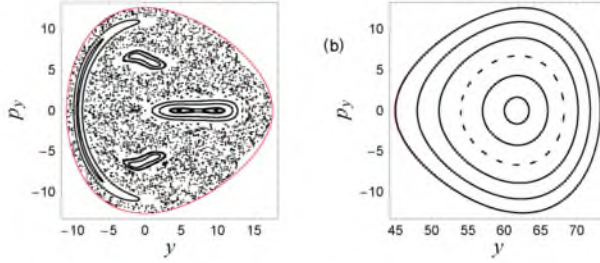


**Fig. 2,b.** Type of motion  $RC$ .  $E = 80.0$ . Shown is the surface of section for central (left) and peripheral (right) local minima

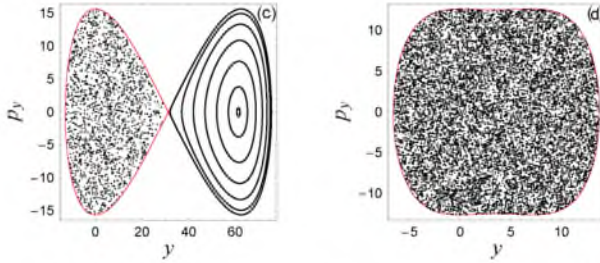


**Fig. 2,c (left).** Type of motion  $RC$ .  $E = V_s = 122.0703125$

**Fig. 2,d (right).** Type of motion  $C$ .  $E = 80.0$

Fig. 2 demonstrates the type of classical motion in three energy regions of interest ( $R$ ,  $RC$ , and  $C$ ). Particularly, mixed state is seen on Fig. 2b, 2c.

### 3. COMPUTATION OF QUANTUM ENERGY SPECTRA

For the purpose of quantum mechanical calculations we consider the Hamiltonian (1) in polar form

$$\hat{H} = -\frac{1}{2} \left( \frac{\partial^2}{\partial r^2} + \frac{1}{r^2} \frac{\partial^2}{\partial \varphi^2} - r^2 \right) + b \frac{r^3}{3} \sin 3\varphi + cr^4. \quad (4)$$

In order to calculate the quantum energy spectra the eigenvalue problem

$$\hat{H}(r, \varphi) \psi(r, \varphi) = E \psi(r, \varphi) \quad (5)$$

should be solved. Eigenvalues of the Hamiltonian (4) were calculated by diagonalizing the Hamiltonian matrix  $\langle N', l' | \hat{H} | N, l \rangle$ . The basis functions  $|N, l\rangle$  were chosen in the form

$$\tilde{u}_{N,l}(r, \varphi) = \frac{1}{\sqrt{2}} \left( u_{N,l}(r, \varphi) + j u_{N,l}^*(r, \varphi) \right), \quad (6)$$

where  $u_{N,l}(r, \varphi)$  are basis functions of the unperturbed harmonic oscillator:

$$u_{N,l}(r, \varphi) = \frac{1}{\sqrt{2\pi}} e^{-il\varphi} R(N, l), \quad j = \pm 1. \quad (7)$$

The value  $R(N, l)$  in (7) is defined as

$$R(N, l) = \sqrt{2\omega} i^N \sqrt{\left( \frac{N-l}{2} \right)!} / \sqrt{\left( \frac{N+l}{2} \right)!} \times \left( \sqrt{\omega} r \right)^{|l|} L_{N-l}^{|l|}(\omega r^2) e^{-\omega r^2/2}, \quad (8)$$

where  $L_n^{|l|}(t)$  is the Laguerre polynomial,  $\omega$  is the fitting parameter,  $l$  is the angular momentum. The following recursion relations can be obtained:

$$rR(N, l) = i \left\{ \sqrt{\frac{N+l}{2}} R(N-1, l-1) + \sqrt{\frac{N-l+2}{2}} R(N+1, l-1) \right\}, \quad (9)$$

$$rR(N, l) = -i \left\{ \sqrt{\frac{N-l}{2}} R(N-1, l+1) + \sqrt{\frac{N+l+2}{2}} R(N+1, l+1) \right\}. \quad (10)$$

It is important to take the full symmetry of the Hamiltonian (4) into account for two reasons: 1) the matrix  $\langle N', l' | \hat{H} | N, l \rangle$  can be divided into submatrices, corresponding to the different irreducible representations of the symmetry group of the Hamiltonian (4) (that allows to calculate the eigenvalues of each type separately); 2) it is necessary to distinguish energy levels of each symmetry type to perform spectral statistical analysis correctly [7].

The full symmetry of the Hamiltonian (4) is the  $C_{3v}$ -point group, which is the symmetry group of an equilateral triangle. It has three irreducible representations:  $A_1$ ,  $A_2$ , and  $E$ . The eigenvalues corresponding to  $A_1$  and  $A_2$  symmetries are generally non-degenerate, while those of  $E$  symmetry are doubly degenerate. Basis functions (6) are classified according

to the irreducible representations of the  $C_{3v}$ -point group as shown in Table 2.

**Table 2.** Classification of the basis functions (5) according to the irreducible representations of the  $C_{3v}$ -point group

Symmetry		$j$	$l$
$A_1$		1	$l = 0 \pmod{3}$
$A_2$		-1	$\begin{cases} l = 0 \pmod{3}, \\ l > 0 \end{cases}$
$E$ :	$E_1$	1	$l \neq 0 \pmod{3}$
	$E_2$	-1	

Using the orthogonality relation  $\int_0^\infty R(N', l)R(N, l)rdr = \delta_{N'N}$  together with the recursion relations (9), (10) we get the explicit formula for matrix elements  $\delta_{nm}$  is the Kronecker delta symbol and  $j = \pm 1$  depending on the type of the symmetry (cf. Table 2).

$$\begin{aligned}
\langle N', l' | \hat{H} | N, l \rangle = & \omega(N+1)\delta_{l'l}\delta_{N'N} - \frac{b}{6\omega^{3/2}} \cdot \frac{1}{2(\delta_{l'0} + \delta_{l'0})/2} \left\{ (j\delta_{l'(l-3)} + \delta_{l'(-l+3)})F(N, l) \right. \\
& + \delta_{l'(l+3)}F(N, -l) \left. \right\} + \delta_{l'l} \frac{c}{\omega^2} \left\{ \frac{1}{4} \sqrt{(N+l)(N-l)(N+l-2)(N-l-2)} \delta_{N'(N-4)} + N \sqrt{(N+l)(N-l)} \delta_{N'(N-2)} \right. \\
& + \left( \frac{3}{2}N^2 - \frac{l^2}{2} + 3N + 2 \right) \delta_{N'N} + (N+2) \sqrt{(N+l+2)(N-l+2)} \delta_{N'(N+2)} + \frac{1}{4} \sqrt{(N+l+2)(N-l+2)} \\
& \times \sqrt{(N+l+4)(N-l+4)} \delta_{N'(N+4)} \left. \right\} + \frac{1-\omega^2}{2\omega} \delta_{l'l} \left\{ \frac{1}{2} \sqrt{(N+l)(N-l)} \delta_{N'(N-2)} + (N+1) \delta_{N'N} \right. \\
& \left. + \frac{1}{2} \sqrt{(N+l+2)(N-l+2)} \delta_{N'(N+2)} \right\}, \quad (11)
\end{aligned}$$

where

$$\begin{aligned}
F(N, l) = & \sqrt{\frac{(N+l)(N+l-2)(N+l-4)}{8}} \delta_{N'(N-3)} + 3 \sqrt{\frac{(N+l)(N-l+2)(N+l-2)}{8}} \delta_{N'(N-1)} \\
& + 3 \sqrt{\frac{(N+l)(N-l+2)(N-l+4)}{8}} \delta_{N'(N+1)} + \sqrt{\frac{(N-l+2)(N-l+4)(N-l+6)}{8}} \delta_{N'(N+3)}. \quad (12)
\end{aligned}$$

In practical calculations the elements of the Hamiltonian matrix were ordered by the value of  $N$ ,  $N = 0, 1, \dots, N_{\max}$ . We calculated matrix elements choosing  $N_{\max} = 250$ , except for  $E$ -symmetry in the region  $C$ , where calculations were performed for  $N_{\max} = 175$ . The matrix  $\langle N', l' | \hat{H} | N, l \rangle$  is banded with the band  $2m+1$ , where  $m$  depends on the quantum number  $N$  as

$$m(N) = \begin{cases} \dim_H(N), & N < 4, \\ \dim_H(N) - \dim_H(N-4) + 1, & N \geq 4, \end{cases} \quad (13)$$

where  $\dim_H(N)$  is dimension of the Hamiltonian matrix for particular  $N$ .

Diagonalization of the Hamiltonian matrix  $\langle N', l' | \hat{H} | N, l \rangle$  was performed using the reduction to the tridiagonal form of symmetric band matrix via Jacobi rotations [8, p. 244] followed by the procedure for calculating specific eigenvalues in given interval of symmetric tridiagonal matrix via the method of bisection [8, p. 367]. We obtained 5334 energy levels of  $A_1$ -type,

5208 levels of  $A_2$ -type in each energy region considered, and we obtained 10542 levels of  $E_1$ -type in the regions  $R$  and  $RC$ , and 5192 levels in the region  $C$ . The accuracy of the results was examined by changing the size of the basis and by varying the fitting parameter  $\omega$  in expressions (8) and (11). The energy levels, reliable with an accuracy  $\Delta < 0.1 \cdot s_{\min}$  ( $s_{\min}$  is the minimum spacing between nearest-neighbor levels) were accepted for further statistical analyses. The error  $\Delta$  is defined as

$$\Delta = \max_i \left\{ \left| a_i^{(N_{\max})} - a_i^{(N_{\max}-1)} \right| \right\}, \quad (14)$$

where  $a_i^{(N_{\max})}$ ,  $a_i^{(N_{\max}-1)}$  are the  $i$ -th energy levels, obtained via the diagonalization of Hamiltonian matrices computed for  $N = N_{\max}$  and  $N = N_{\max} - 1$  respectively.

#### 4. STATISTICAL PROPERTIES OF SPECTRAL FLUCTUATIONS

Spectral statistical analysis is applied to spectral fluctuations, i.e. spectrum deviations from its smooth (locally uniform) behavior [1,9]. The distribution func-

tion (the staircase function)  $N(E)$  for a discrete spectrum can be written as

$$N(E) = N_{av}(E) + N_{fluct}(E), \quad (15)$$

where  $N_{av}(E)$  is the average part and  $N_{fluct}(E)$  is the fluctuation part of the staircase function. Since the smooth behavior is not universal, it is removed by the spectrum “unfolding” procedure via the mapping

$$x_n + 1/2 = N_{av}(E_n). \quad (16)$$

We calculated  $N_{av}(E)$  in terms of the few lower-order spectral moments by using a truncated Gram-Charlier expansion [10] for the distribution function  $F(x)$  of the normalized quantity  $x = (E - m_E)/\sigma$  ( $m_E$  is the expectation,  $\sigma$  is the standard deviation of the spectrum  $\{E_i\}$ ).

The following statistical properties of the system (4) were investigated: 1) the distribution  $p(s)$  of spacing  $s$  between nearest-neighbor levels of the spectrum; and 2) the Dyson’s  $\Delta_3$ -statistic which measures the spectral rigidity and is defined by

$$\Delta_3(\alpha; L) \equiv \frac{1}{L} \min_{A,B} \int_{\alpha}^{\alpha+L} [N(x) - (Ax+B)]^2 dx, \quad (17)$$

$$\Delta_3(L) = \langle \Delta_3(\alpha_i, L) \rangle. \quad (18)$$

The following theoretical predictions are known [1,2]:

(1)  $p(s) = \exp(-s)$  (Poisson distribution) and  $\Delta_3(L) \sim L/15$  for integrable classical systems;

(2)  $p(s) \approx As^\beta \exp(-Bs^2)$  and  $\Delta_3(L) \sim \gamma \ln L + \delta$  for chaotic systems. Particularly,

$p(s) \approx \pi s/2 \exp(-\pi s^2/4)$  (Wigner distribution) and  $\Delta_3(L) \sim 1/\pi \ln L - 0.00695$  for systems with quantum spectrum well described by random matrix theory, namely by statistical properties of the Gaussian orthogonal ensemble (GOE);

(3) In case of a generic system where regular and chaotic trajectories coexist, distribution  $p(s)$  may well be fitted by Brody distribution

$$p_q(s) = \alpha s^q \exp(-\beta s^{1+q}), \quad (19)$$

$$\alpha = (1+q)\beta, \quad \beta = [\Gamma((2+q)/(1+q))]^{1+q}, \quad (20)$$

Note that with  $q \rightarrow 0$   $p_q(s)$  approaches Poisson distribution, and with  $q \rightarrow 1$   $p_q(s)$  approaches Wigner distribution.

## 5. RESULTS AND CONCLUSIONS

Since the results obtained for different symmetry types are qualitatively the same, only the results for  $E$ -symmetry type are given. The solid line on pictures below is used to display the predictions for regular system, the dashed line is for the predictions for chaotic system.

As can be seen from Fig. 3, regularity of the classical motion in the  $R$  region is approved by the statistical

properties of the fluctuations of spectra. Namely,  $p(s)$  is close to the Poissonian distribution, while  $\Delta_3(L) \sim L/15$  in the range  $0 \leq L \leq L_{\max}$ , and  $\Delta_3(L)$  “saturates” after that – i.e. all the classical trajectories complement to the value of  $\Delta_3(L)$ , and  $\Delta_3(L)$  moves away from straight line and fluctuates about some value  $\Delta_\infty$ , which is not universal. Figs. 4 and 5 present the results for mixed  $RC$  region.

### REGION R

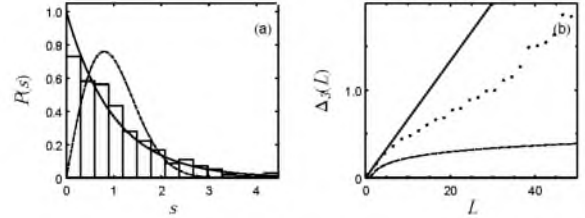


**Fig. 3.**  $E_1$ -type. Total number of levels – 701 (levels from 5000 to 5700,  $E_{5000} \approx 171.7$ ,  $E_{5700} \approx 183.2$ ), number of bins in the histogram – 15;  $\Delta_3(L)$  is the ensemble average (levels from 4950 to 5650, from 5000 to 5700, and from 5050 to 5750)

### REGION RC

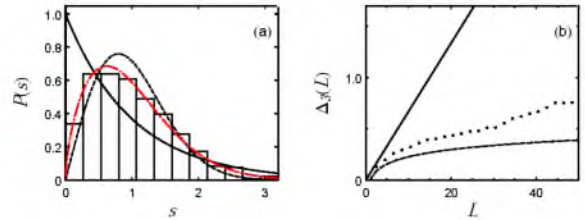


**Fig. 4.**  $E_1$ -type. Total number of levels – 501 (levels from 1380 to 1880,  $E_{1380} \approx 87.7$ ,  $E_{1880} \approx 101.5$ ), number of bins in the histogram – 12;  $\Delta_3(L)$  is the ensemble average (levels from 1320 to 1820, from 1350 to 1850, and from 1380 to 1880). Dash-dotted line is the Brody distribution (19)-(20) with  $q \approx 0.6262$

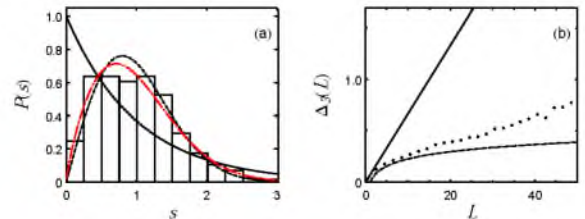


**Fig. 5.**  $E_1$ -type. Total number of levels – 501 (levels from 1680 to 2180,  $E_{1680} \approx 96.2$ ,  $E_{2180} \approx 108.7$ ), number of bins in the histogram – 12;  $\Delta_3(L)$  is the ensemble average (levels from 1620 to 2120, from 1650 to 2150, and from 1680 to 2180). Dash-dotted line is the Brody distribution (22) with  $q \approx 0.7858$

The more the levels in the analysis get close to the saddle energy  $V_s$  (particularly,  $V_s = 122.0703125$ ), the

more the properties of  $p(s)$  and  $\Delta_3(L)$  get close to the theoretical predictions for chaotic systems. Parameter  $q$  in Brody distribution (19)-(20) in this case tends to unity.

As it is seen from Fig. 6 the spectrum in the region  $C$  is well described by the properties of Gaussian orthogonal ensemble (GOE) of random matrices what goes along with the theoretical predictions for chaotic systems.

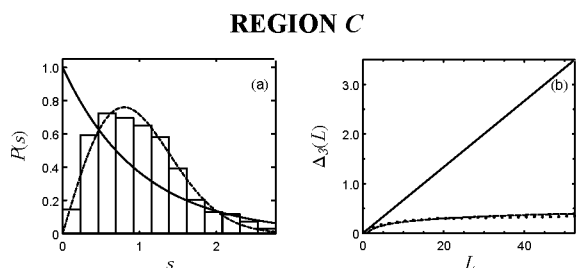


**Fig. 6.**  $E_1$ -type. Total number of levels – 301 (levels from 490 to 790,  $E_{490} \approx 58.3$ ,  $E_{790} \approx 79.9$ ), number of bins in the histogram – 12;  $\Delta_3(L)$  is the ensemble average (levels from 440 to 740, from 465 to 765, and from 490 to 790)

In present investigation we were searching for quantum signatures of classical chaos in a system with non-trivial topology of the potential. We found that statistical properties of spectra of the system with complex topology of the potential such as system (1) are in agreement with the theory developed for integrable, chaotic and generic (neither regular nor chaotic) systems.

## REFERENCES

1. O. Bohigas, M.J. Giannoni. Chaotic motion and random-matrix theory // *Lecture Notes in Physics*. 1984, v. 209, p. 1871-1969.
2. M.V. Berry. Classical Chaos and Quantum Eigenvalues // *Order and Chaos in nonlinear physical systems* (ed. S. Lundquist, N. March and M. Tosti). New York and London: Plenum Press, 1988, p. 340-348.
3. S.W. McDonald, A.N. Kaufman. Spectrum and Eigenfunctions for a Hamiltonian with Stochastic Trajectories // *Phys. Rev. Lett.* 1979, v. 42, p. 1189-1191.
4. A. Matsuyama. Numerical study of the quantum mechanical Toda lattice // *Phys. Lett.* 1991, v. A161, p. 124-129.
5. V.P. Berezovoj, Yu.L. Bolotin, V.A. Cherkaskiy. arXiv:nlm. CD/0311012, 2003, v. 2, p. 19.
6. Yu.L. Bolotin, V.Yu. Gonchar, V.N. Tarasov, N.A. Chekanov. The transition regularity-chaos-regularity and statistical properties of wave function // *Phys. Lett.* 1990, v. A144, N8,9, p. 459-461.
7. Yu.L. Bolotin, S.I. Vinitisky, V.Yu. Gonchar et al. *Projavenie stokhastichnosti v spektrakh nekotorykh gamiltonovykh system s diskretoi simmetriei*: Preprint JNR, P4-89-590, Dubna, 1989, 26 p. (in Russian).
8. J.H. Wilkinson, C. Reinsch. Handbook for automatic computation, v. 2: Linear algebra. New York, Springer-Verlag, 1971 (in Russian).
9. T.A. Brody, J. Flores, J.B. French, P.A. Mello, A. Pandey, and S.M. Wong. Random-matrix physics: spectrum and strength fluctuations // *Rev. Mod. Phys.* 1981, v. 53, p. 385-479.
10. H. Cramer. *Mathematical methods of statistics*. Stockholm: University press, 1946.

## СВОЙСТВА СПЕКТРА ДВУМЕРНОГО МНОГОЯМНОГО СЗВ СИММЕТРИЧНОГО ГАМИЛЬТОНИАНА

*Н.А. Чеканов, Е.В. Шевченко*

Рассмотрена квантовая гамильтонова система, поверхность потенциальной энергии которой имеет четыре локальных минимума и которая в классическом пределе допускает в некотором интервале энергий смешанное состояние. Для данной системы методом диагонализации вычислен энергетический спектр, распределение расстояний между соседними уровнями и  $\Delta_3$ -жесткость Дайсона. Полученные результаты сопоставлены с теоретическими предсказаниями для регулярных, хаотических систем и систем, в которых регулярные и хаотические траектории сосуществуют.

## ВЛАСТИВОСТІ СПЕКТРУ ДВОВИМІРНОГО БАГАТОЯМНОГО СЗВ СИМЕТРИЧНОГО ГАМИЛЬТОНІАНУ

*М.О. Чеканов, Є.В. Шевченко*

Розглянуто квантову гамільтонову систему, поверхня потенційної енергії якої має чотири локальних мінімуми, і яка в класичній межі допускає в деякому інтервалі енергій змішаний стан. Для даної системи методом діагоналізації обчислений енергетичний спектр, розподіл відстаней між сусідніми рівнями й  $\Delta_3$ -жорсткість Дайсона. Отримані результати зіставлені з теоретичними передбаченнями для регулярних, хаотичних систем і систем, в яких регулярні й хаотичні траекторії співіснують.